

# Inactivation of the 14-3-3 $\sigma$ Gene Is Associated with 5' CpG Island Hypermethylation in Human Cancers<sup>1</sup>

Hiromu Suzuki, Fumio Itoh,<sup>2</sup> Minoru Toyota, Takefumi Kikuchi, Hideki Kakiuchi, and Kohzoh Imai

First Department of Internal Medicine, Sapporo Medical University, Sapporo 060-8543, Japan

## Abstract

The cell cycle checkpoint plays an important role in maintaining the integrity of cells. Recently, one of the 14-3-3 protein family members, 14-3-3 $\sigma$ , was shown to be regulated by p53 and to play a role in the G<sub>2</sub>-M-phase checkpoint. To determine whether 14-3-3 $\sigma$  is inactivated in human cancers, the methylation status of the 5' region of 14-3-3 $\sigma$  was investigated in a series of gastric, colorectal, and hepatocellular cancer cell lines. Of 22 cell lines examined, 6 showed aberrant methylation. The methylation status of 14-3-3 $\sigma$  was found to be correlated with loss of expression, which was restored by 5-aza-2'-deoxycytidine treatment. Furthermore, normal G<sub>2</sub> arrest after DNA damage was not demonstrated in the cell lines with methylation. In primary gastric cancers, 14-3-3 $\sigma$  hypermethylation was observed frequently in 26 of 60 (43%) cases and observed more frequently in poorly differentiated adenocarcinomas ( $P = 0.0017$ ). Our findings suggest that 14-3-3 $\sigma$  is inactivated by aberrant methylation of the 5' region in various human cancers and that it might play an important role in the development of undifferentiated gastric cancers.

## Introduction

Members of the ubiquitous and highly conserved 14-3-3 protein family modulate a wide variety of cellular processes, such as preventing apoptosis in association with a Bcl-2 family member, BAD (1, 2), and the G<sub>2</sub> checkpoint control binding with Cdc25C (3, 4). The  $\sigma$  isoform of 14-3-3 (also called stratifin or HME-1) is expressed in keratinocytes (5) and epithelial cells (6). 14-3-3 $\sigma$  has been shown to be associated with growth regulation and signal transduction (6, 7) as well as with cellular dedifferentiation (8), although its function has not been elucidated. Recently, Hermeking *et al.* (9) reported that expression of 14-3-3 $\sigma$  mRNA was induced in a p53-dependent manner in response to DNA damage caused by  $\gamma$ -irradiation and DNA-damaging agents, and overexpression of 14-3-3 $\sigma$  blocks the cell cycle at the G<sub>2</sub> phase. More recently, 14-3-3 $\sigma$  has been shown to prevent mitotic catastrophe, indicating that 14-3-3 $\sigma$  plays an important role in the G<sub>2</sub> checkpoint (10). Despite the putative tumor suppressor activity of 14-3-3 $\sigma$ , mutations or loss of the gene in human cancers have not been reported. In the present study, we investigated the aberrant methylation of the 5' region of the 14-3-3 $\sigma$  gene in a series of GC,<sup>3</sup> CRC, and HCC cell lines. Six of the cell lines showed aberrant methylation, and the methylation correlated well with the loss of 14-3-3 $\sigma$  mRNA expression. Methylation of 14-3-3 $\sigma$  was also observed in primary

GCs, and a strong correlation between methylation and a poorly differentiated histological phenotype was observed. To investigate methylation, we performed a combination of bisulfite treatment and fluorescence PCR-SSCP. PCR products from bisulfite-treated DNA were electrophoresed in nondenaturing polyacrylamide gels, and methylated and unmethylated alleles were readily detected due to the different mobility caused by different conformations (11). This novel procedure can provide information about the methylation level of the gene and is quite easy to adapt to a large number of samples.

## Materials and Methods

**Cell Lines and Cancer Tissue Samples.** GC cell lines (MKN28, MKN45, MKN74, AZ521, NUGC3, JRST, and KatoIII), CRC cell lines (DLD1, HT29, HCT116, BM314, WiDr, Colo201, Colo205, and Colo320DM), and HCC cell lines (CHC4, CHC20, CHC32, Chang, and PLC/PRF/5) were cultured in RPMI1640 supplemented with 10% FCS. HCC cell lines (RKO, HLE, and HuH7) were cultured in DMEM supplemented with 10% FCS. Fresh frozen tumor tissue samples of GCs were obtained from surgical resections. A series of GC xenograft tissues was established in our laboratory by implanting fresh surgically resected tissues into severe combined immunodeficient (SCID) mice dorsally. Genomic DNAs were extracted from the cell lines and tumor tissues by a standard phenol/chloroform procedure. Total RNA was extracted from the cell lines and xenograft tissues by using a RNA extraction kit, Sepagene (Nippon Gene Co., Tokyo, Japan).

**Bisulfite Modification.** Bisulfite modification was performed as described previously (12). Briefly, approximately 2  $\mu$ g of genomic DNA were denatured in 0.2 M NaOH for 10 min. Sodium bisulfite (Sigma, St. Louis, MO) was added to a final concentration of 3.1 M, and hydroquinone (Sigma) was added to a final concentration of 0.5 mM. The reaction was performed at 50°C for 16 h. Modified DNA was purified using Wizard DNA purification resin (Promega) according to the manufacturer's recommendations and eluted into 50  $\mu$ l of water. Modification was completed by NaOH (final concentration, 0.3 M) treatment for 5 min at room temperature, followed by ethanol precipitation.

**Bisulfite Genomic Sequencing Analysis.** Sodium bisulfite-modified genomic DNA was PCR amplified by using two primer pairs specific for the 5' region of the 14-3-3 $\sigma$  gene: (a) the sequence that includes the transcription start site (region 1); and (b) the subsequent sequence (region 2). Region 1 corresponds to -220 to +116, and region 2 corresponds to +93 to +350 (Fig. 1A). PCR reactions were performed in a volume of 50  $\mu$ l containing 1  $\times$  PCR buffer (Takara, Tokyo, Japan), 0.25 mM dNTP, 1  $\mu$ M of each primer, and 2.5 units of Taq polymerase (Takara). PCR conditions were 95°C for 5 min and 35 cycles at 95°C for 30 s, 53°C for 30 s, and 72°C for 30 s for region 1 amplification and 35 cycles at 95°C for 30 s, 56°C for 30 s, and 72°C for 30 s for region 2. In all PCRs, polymerase was added after the heat block had reached 95°C to effect a hot start of the amplification. Primer sequences are as follows: (a) 5'-AAAGGTGTTAGTG-TAGGTGGGGTT-3' (region 1, sense primer); (b) 5'-CCTACTCTACCAACT-TAACCTTCT-3' (region 1, antisense primer); (c) 5'-AGAAGGTTAAGTTGG-TAGAGTAGG-3' (region 2, sense primer); and (d) 5'-CCTAAAACCTCAAT-CTCCACCTTCT-3' (region 2, antisense primer). Amplified PCR products were cloned by using the pGEM-T Easy Vector System (Promega, Madison, WI). Plasmid DNAs were purified with the QIAfilter Midiprep Kit (Qiagen, Hilden, Germany). Sequence reactions were performed by using the Auto Read Sequencing Kit (Pharmacia Biotech, Uppsala, Sweden). Samples were loaded onto 6%

Received 12/10/99; accepted 6/26/00.

The costs of publication of this article were defrayed in part by the payment of page charges. This article must therefore be hereby marked *advertisement* in accordance with 18 U.S.C. Section 1734 solely to indicate this fact.

<sup>1</sup> Supported by a grant-in-aid from the Ministry of Education, Science, Sports and Culture (to F. I. and K. I.). M. T. was a postdoctoral fellow from Japan Society for the Promotion of Science. H. S. and F. I. contributed equally to this work.

<sup>2</sup> To whom requests for reprints should be addressed, at First Department of Internal Medicine, Sapporo Medical University, S-1, W-16, Chuo-ku, Sapporo, 060-8543, Japan. Fax: 81-011-613-1141; E-mail: fitoh@sapmed.ac.jp.

<sup>3</sup> The abbreviations used are: GC, gastric cancer; CRC, colorectal cancer; HCC, hepatocellular cancer; SSCP, single-strand conformational polymorphism; RT, reverse transcription; dNTP, deoxynucleotide triphosphate; CIN, chromosomal instability.

urea-polyacrylamide denaturing gels in an ALF express automated DNA sequencer (Pharmacia Biotech). Five to 10 clones were sequenced for each cell line.

**Bisulfite-SSCP Analysis.** For SSCP analysis, two regions of the *14-3-3 $\sigma$*  gene were PCR amplified with the same primer sequences described above, of which each sense primer was end-labeled with Cy5. One  $\mu$ l of fluorescent products was diluted with 10  $\mu$ l of loading dye (95% formamide, 20 mM EDTA, 0.05% xylene cyanol, and 0.05% bromophenol blue), heat denatured for 5 min at 95°C, cooled on ice for 5 min, and loaded onto 5% polyacrylamide nondenaturing gel (99:1 acrylamide to bisacrylamide) containing 5% glycerol in an ALF express automated DNA sequencer (Pharmacia Biotech). Electrophoresis was performed for 400 min, and during electrophoresis, the gel was kept at 30°C with a circulator instrument. Obtained data were analyzed using Fragment Manager Software (Pharmacia Biotech). Details of the protocol are as reported previously (11).

**Northern Blot Analysis.** A 375-bp probe specific for the 3' region of the *14-3-3 $\sigma$*  gene was generated by PCR amplification as described previously (9). The PCR product was cloned and sequenced, and it was verified to be consistent with *14-3-3 $\sigma$* . The probe was labeled with  $^{32}$ P dCTP by using the Random Primer Labeling Kit (Takara) and hybridized at 42°C, followed by analysis using an autoradiograph instrument (BAS2000; Fuji Film, Tokyo, Japan).

**5-Aza-2'-deoxycytidine Treatment.** Cell lines that did not express *14-3-3 $\sigma$*  were treated with 5-aza-2'-deoxycytidine (Sigma) that was dissolved in cold RPMI1640 immediately before use. Cells were grown in a medium containing 5  $\mu$ M 5-aza-2'-deoxycytidine for 5 days, and the medium and drug were replaced every 24 h.

**mRNA-selective PCR.** RT-PCR for *14-3-3 $\sigma$*  was performed by using the mRNA-selective PCR kit (Takara). RT reactions were performed in a volume of 50  $\mu$ l containing 1  $\times$  mRNA-selective PCR buffer, 5 mM MgCl<sub>2</sub>, 1 mM dNTP/analogous mixture, 0.8 unit/ $\mu$ l RNase inhibitor, 0.1 unit/ $\mu$ l avian myeloblastosis virus reverse transcriptase XL, 1  $\mu$ M oligo (dT) primer, and 1  $\mu$ g of total RNA. The RT conditions were 30°C for 10 min, 42°C for 30 min, and 5°C for 5 min. Subsequent PCR reactions were performed in a volume of 50  $\mu$ l containing 1  $\times$  mRNA-selective PCR buffer, 5 mM MgCl<sub>2</sub>, 1 mM dNTP/analogous mixture, 0.1 unit/ $\mu$ l avian myeloblastosis virus-optimized Taq, 0.4  $\mu$ M of each primer, and 10  $\mu$ l of the RT reactant. The PCR conditions were 25 cycles at 85°C for 1 min, 58°C for 1 min, and 72°C for 1 min. Because cDNA generated by the RT reaction contained dNTP analogues and was denatured at 85°C, contaminating genomic DNA should not be amplified in the PCR reaction. For *14-3-3 $\sigma$*  mRNA amplification, the same primer sequences used for generating the Northern blot probe were used. The integrity of RNA was evaluated by amplification of human *GAPDH* mRNA. Primer sequences for *GAPDH* were 5'-CAGCCGAGCCACATCG-3' (sense) and 5'-TGAGGCTGTTGTCATACTTCTC-3' (antisense).

**Genomic PCR Amplification.** Twenty-two cell lines listed above were examined for mutation by DNA sequencing. The PCR reaction was performed in a volume of 50  $\mu$ l containing 1  $\times$  PCR buffer, 0.25 mM dNTP, 1  $\mu$ M of each primer, and 2.5 units of Taq polymerase at 95°C for 5 min and 35 cycles at 95°C for 1 min, 68°C for 1 min, and 72°C for 1 min. Primer sequences specific for the *14-3-3 $\sigma$*  gene were 5'-AGAGACACAGAGTCCGGCATTGGTC-CCAGGCAGCA-3' (sense) and 5'-ACCCCATAGTCTCTCGGCA-GGGTGGGGGACT-3' (antisense). Amplified PCR products were cloned by using the pGEM-T Easy Vector System (Promega) and sequenced as described above.

**Flow Cytometry Analysis.** Cells were rinsed in PBS buffer, trypsinized, collected by centrifugation, and stained by propidium iodide (Sigma). Flow cytometry was performed with a FACScan instrument (Becton Dickinson, San Jose, CA).

**Mutation Analysis of p53.** To detect mutations of *p53*, SSCP was performed for exons 5–8. PCR was performed as described previously (13). Sense primers were end labeled with Cy5. For SSCP, 1  $\mu$ l of PCR products was mixed with 10  $\mu$ l of loading buffer, denatured at 95°C for 5 min, cooled on ice for 5 min, and electrophoresed in 5% polyacrylamide nondenaturing gels as described above. The presence of abnormally migrating bands was confirmed by four different conditions (with 5% glycerol at 15°C, 20°C, 25°C, and 30°C).

**Statistical Analysis.** Statistical comparisons were performed using Fisher's exact test.

## Results

**Methylation Analysis of the *14-3-3 $\sigma$*  5' CpG Island in Tumor Cell Lines.** The *14-3-3 $\sigma$*  gene has a CpG island that spans approximately 850 bp. This area has a 65% GC content, and the CpG:GpC ratio is 0.53, which fulfills the criteria for a CpG island (14). This island is unique in the sense that the transcription start site is located at the 5' edge of the island, and the most CpG-rich area is in the coding region of the gene. We investigated the methylation status of the 5' region of *14-3-3 $\sigma$*  in 7 GC, 8 CRC, and 7 HCC cancer cell lines. Genomic DNA extracted from the cell lines was treated with sodium bisulfite, followed by PCR amplification of the 5' region of the *14-3-3 $\sigma$*  gene. Because unmethylated cytosine residues were converted to thymine, whereas methylated cytosine residues were resistant to bisulfite modification, different sequences should be created according to the methylation status. The 5' region that encompasses the transcription start site and the subsequent region (regions 1 and 2 in Fig. 1A) were amplified and analyzed by bisulfite-SSCP (Fig. 1B). Two GC cell lines (MKN28 and MKN74), one CRC cell line (Colo320DM), and three HCC cell lines (Chang, HLE, and HuH7)

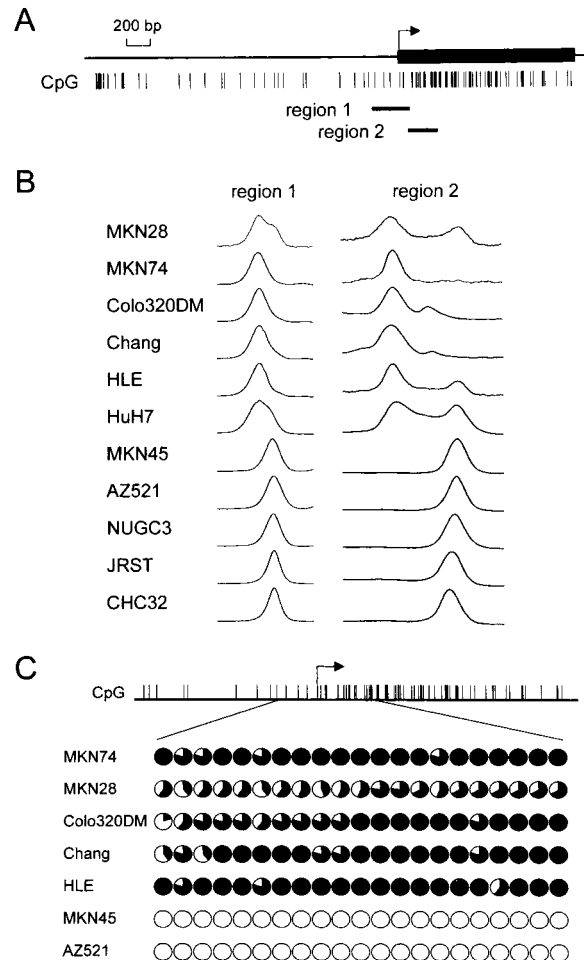


Fig. 1. Aberrant methylation of the 5' CpG island of *14-3-3 $\sigma$*  in tumor cell lines. **A**, schematic representation of the 5' CpG island of *14-3-3 $\sigma$*  is shown. An exon of *14-3-3 $\sigma$*  is indicated by a solid bar. The transcription start site is indicated by an arrow. CpG sites are indicated by vertical bars. The regions examined for methylation are shown below. **B**, detection of methylation of *14-3-3 $\sigma$*  using bisulfite-SSCP analysis. The cell lines examined are shown on the left. A distinct band shift is observed in MKN28, MKN74, Colo320DM, Chang, HLE, and HuH7. **C**, summary of the bisulfite sequence in cell lines with or without *14-3-3 $\sigma$*  methylation. In total, 21 CpG sites around the transcription start site were examined by bisulfite sequencing. The methylated CpG sites are indicated by solid circle, and the unmethylated CpG sites are indicated by open circle. The cell lines examined are shown on the left.

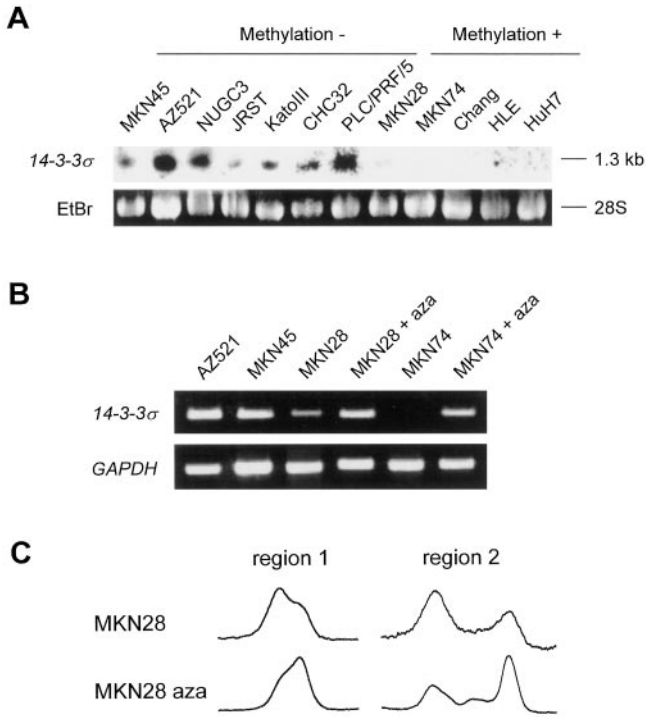


Fig. 2. Expression analysis of *14-3-3 $\sigma$*  in various tumor cell lines by Northern blot. Twenty  $\mu$ g of total RNA were electrophoresed, blotted, and transferred to nylon membranes. A 375-bp fragment of DNA of *14-3-3 $\sigma$*  was labeled with [ $^{32}$ P]dCTP and hybridized with membranes. Cell lines with *14-3-3 $\sigma$*  methylation (MKN28, MKN74, Chang, HLE, and HuH7) showed no or only negligible levels of expression (A). Reexpression of *14-3-3 $\sigma$*  after 5-aza-2'-deoxycytidine treatment by selective mRNA PCR (B). aza, 5-aza-2'-deoxycytidine treatment. The band size of *14-3-3 $\sigma$*  is 375 bp. GAPDH was amplified to examine the integrity of mRNA. Demethylation of the 5' CpG island of *14-3-3 $\sigma$*  in MKN28 by 5-aza-2'-deoxycytidine treatment is shown (C). Methylation statuses of regions 1 and 2 were examined by bisulfite-SSCP before and after 5-aza-2'-deoxycytidine treatment in MKN28. After treatment, the peak of shifted bands was reduced for both regions 1 and 2.

showed aberrant peaks compared with other cell lines. The PCR products were cloned, and cumulative data derived from sequence information from multiple clones revealed that the 5' CpG island of *14-3-3 $\sigma$*  was densely methylated in these cell lines except for MKN28, which was heterogeneously methylated (Fig. 1C).

**Expression and Genomic Sequence Analysis of *14-3-3 $\sigma$* .** We investigated the expression level of the *14-3-3 $\sigma$*  mRNA in 8 GC and 5 HCC cell lines (Fig. 2A). Five cell lines methylated for *14-3-3 $\sigma$*  showed no or only a negligible level of expression. Seven cell lines that are not methylated expressed *14-3-3 $\sigma$*  at various levels. To demonstrate the reexpression of *14-3-3 $\sigma$*  mRNA by a demethylating agent, we performed mRNA-selective PCR. Reduced expression and lack of expression were found in MKN28 and MKN74, respectively, and the expression of *14-3-3 $\sigma$*  was restored in both cell lines after 5-aza-2'-deoxycytidine treatment (Fig. 2B). Demethylation of regions 1 and 2 was observed by bisulfite-SSCP and bisulfite sequencing, confirming that loss of expression is associated with the 5' CpG island hypermethylation (Fig. 2C; data not shown). PCR amplifications specific for the genomic coding region revealed that no deletion of the *14-3-3 $\sigma$*  gene was detected in the 7 GC and 7 HCC cell lines (data not shown). The PCR products were cloned and sequenced, and no mutation was demonstrated.

**Methylation Analysis of *14-3-3 $\sigma$*  in Primary Gastric Cancers.** Next, methylation statuses of *14-3-3 $\sigma$*  were examined in a series of 60 GC cases by bisulfite-SSCP. Tissue samples that showed the same peaks as those of methylated cell lines were presumed to have *14-3-3 $\sigma$*  methylation (see the examples in Fig. 3A). Twenty-six of 60

(43%) cases showed aberrant methylation of regions 1 and 2. Five additional cases (two poorly and three moderately differentiated carcinomas) showed methylation only in region 1. We also performed bisulfite sequencing for 5 of the 26 methylated cases and obtained concordant results (data not shown). We then analyzed the correlation of *14-3-3 $\sigma$*  methylation and the clinicopathological features of the tumors. For statistical analysis, we defined those tumors with both region 1 and 2 methylation as methylated cases. Methylation of *14-3-3 $\sigma$*  was found preferentially in undifferentiated tumor types (1 of 12 well-differentiated adenocarcinomas versus 17 of 31 poorly differentiated adenocarcinomas,  $P = 0.0017$ ; Fig. 3B). The mean age of patients with methylated tissues was  $59.37 \pm 7.95$  years, and the mean age of patients without methylation was  $69.50 \pm 8.52$  years, demonstrating that *14-3-3 $\sigma$*  methylation is not merely an age-related phenomenon. Because good-quality RNA was not available from our primary tumor samples, we investigated *14-3-3 $\sigma$*  mRNA expression in five GC xenograft tissues established in our laboratory. Examples of the methylation analysis of the xenografts are also shown in Fig. 3A. To avoid amplification from contaminated genomic DNA, we performed mRNA-selective PCR. As shown in Fig. 3C, all three xenograft tissues with *14-3-3 $\sigma$*  methylation showed no expression, and two xenografts without *14-3-3 $\sigma$*  methylation expressed the gene.

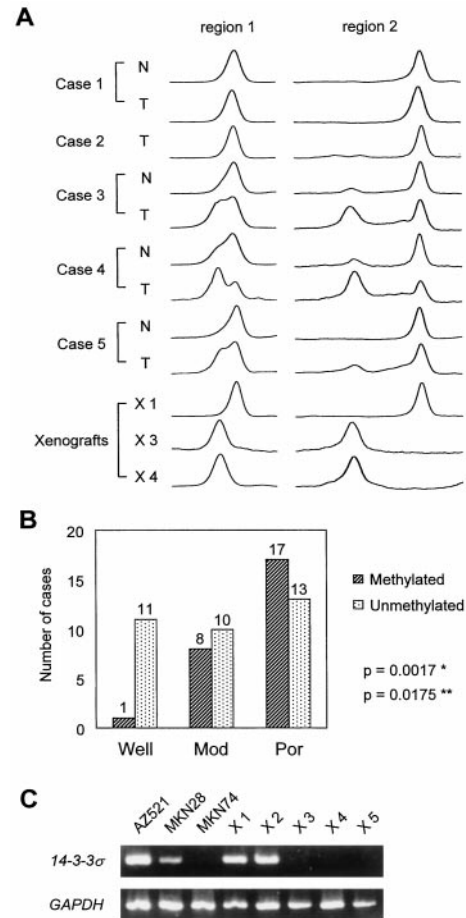


Fig. 3. Aberrant methylation and loss of expression of *14-3-3 $\sigma$*  in primary GCs. A, representative results of bisulfite-SSCP analysis for primary GCs (T<sub>1</sub>-T<sub>4</sub>), GC xenografts (X<sub>1</sub>-X<sub>3</sub>), and noncancerous gastric mucosa (N<sub>1</sub> and N<sub>2</sub>). B, summary of the frequency of *14-3-3 $\sigma$*  methylation in different types of gastric tumors. Well, Mod, and Por denote well, moderately, and poorly differentiated adenocarcinomas, respectively. \*,  $P = 0.0017$  for association of methylation with well-differentiated cases versus poorly differentiated cases. \*\*,  $P = 0.0175$  for association of methylation with well-differentiated cases versus moderately differentiated cases. C, expression analysis of *14-3-3 $\sigma$*  in GC cell lines and xenografts by mRNA-selective PCR. Cell lines and xenografts (X<sub>1</sub>-X<sub>5</sub>) are indicated at the top. Xenografts 3-5 have methylated *14-3-3 $\sigma$*  and show lack of expression.

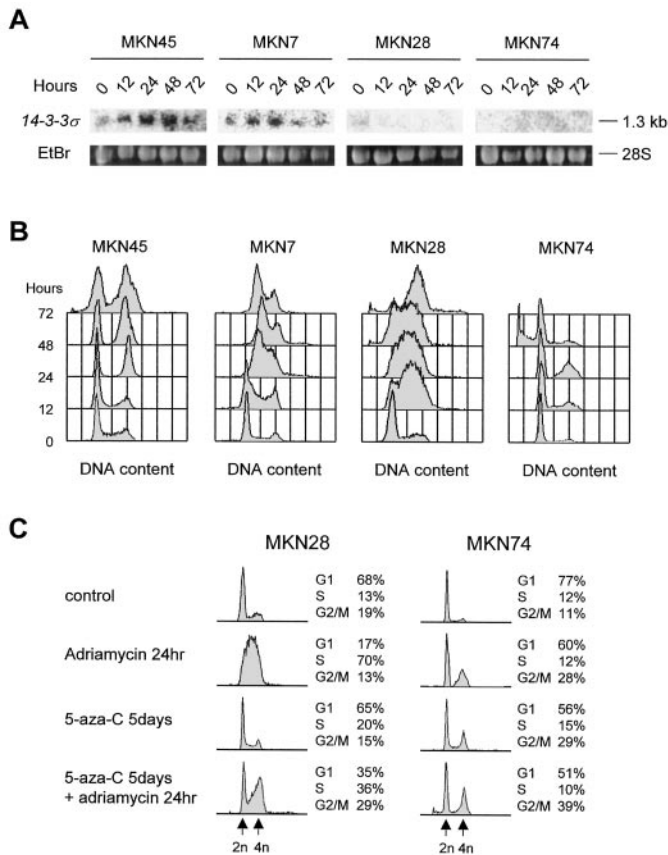


Fig. 4. Absence of *14-3-3 $\sigma$*  in gastric cancer cells is associated with impairment of the  $G_2$  checkpoint. **A**, expression analysis of *14-3-3 $\sigma$*  after treatment with a DNA-damaging agent in cell lines with or without *14-3-3 $\sigma$*  methylation. RNA was prepared at the indicated time after treatment with 0.25  $\mu$ g/ml Adriamycin. Increased expression of *14-3-3 $\sigma$*  was observed in an unmethylated cell line, MKN45. Increased expression was also seen in MKN7, but the expression was reduced after 48 h. **B**, flow cytometry analysis of the cell lines. After treatment with Adriamycin, half of the MKN45 cells showed  $G_2$  arrest. MKN7 showed only partial  $G_2$ -M-phase arrest. MKN28 did not show  $G_2$  arrest until 74 h after treatment. MKN74 began to accumulate in the  $G_2$ -M phase, but apoptosis occurred in most of the cells, and they became extinct after 72 h. **C**, MKN28 and MKN74 cells were treated with 5  $\mu$ M 5-aza-2'-deoxycytidine and then treated with Adriamycin for 24 h and analyzed by flow cytometry. Quantitations of  $G_1$ , S-phase,  $G_2$  cells are indicated on the right. Restoration of  $G_2$  arrest induced by DNA damage was present in MKN28 and MKN74 after 5-aza-2'-deoxycytidine treatment.

In 10 cases, we also investigated the methylation status of noncancerous gastric tissues (Fig. 3A). Five cases that had no methylation in the cancer tissues did not show *14-3-3 $\sigma$*  methylation in their noncancerous gastric tissues. In the remaining five cases with methylated GC tissues, a slight amount of methylation was observed in their noncancerous tissues, although the methylation levels were lower than those seen in the cancer tissues.

A small number of CRC tissue samples ( $n = 17$ ) were also investigated. However, we found no methylation of *14-3-3 $\sigma$*  in these cases (data not shown).

***14-3-3 $\sigma$*  Expression and Cell Cycle Analysis.** It was shown previously that loss of the *14-3-3 $\sigma$*  gene is correlated with impairment of the  $G_2$  checkpoint in CRC cell lines (9, 10). To elucidate the role of aberrant methylation of *14-3-3 $\sigma$*  in GC cell lines, we performed cell cycle analyses in the cell lines with and without *14-3-3 $\sigma$*  methylation. The cell lines examined were MKN45 (*p53* wild type and *14-3-3 $\sigma$*  unmethylated), MKN7 (*p53* mutated and *14-3-3 $\sigma$*  unmethylated), MKN74 (*p53* wild type and *14-3-3 $\sigma$*  methylated), and MKN28 (*p53* mutated and *14-3-3 $\sigma$*  methylated). The cell lines were treated with 0.25  $\mu$ g/ml Adriamycin, followed by Northern blot and flow cytometry analyses at 0–72 h after treatment. As shown in Fig. 4, **A** and **B**,

strong induction of the *14-3-3 $\sigma$*  mRNA and accumulation in  $G_2$  phase was demonstrated in MKN45. MKN7 also showed increased expression of *14-3-3 $\sigma$*  at 12 and 24 h after Adriamycin treatment and showed partial accumulation in  $G_2$  phase. MKN28 did not express *14-3-3 $\sigma$*  and did not show  $G_2$  accumulation until 72 h after treatment. MKN74 was quite fragile to Adriamycin treatment. A small portion of MKN74 cells began to accumulate in the  $G_2$  phase, but apoptosis occurred in most of the cells, and they became extinct after 72 h (Fig. 4B).

To further characterize the role of aberrant methylation of *14-3-3 $\sigma$*  in GC cells, MKN28 and MKN74 were treated with 5-aza-2'-deoxycytidine, followed by treatment with Adriamycin (Fig. 4C). After treatment with 5-aza-2'-deoxycytidine, the *14-3-3 $\sigma$*  mRNA was reexpressed, and the population of cells in  $G_2$  phase after Adriamycin treatment was increased (13% to 29% in MKN28 and 28% to 39% in MKN74), indicating that  $G_2$  arrest induced by DNA damage was partially restored in these cell lines. These results indicated the involvement of *14-3-3 $\sigma$*  methylation in the impairment of the  $G_2$  checkpoint. Consistent results were obtained by the independent, repeated experiments.

**Association Between *14-3-3 $\sigma$*  Methylation and *p53* Mutation.** To elucidate whether methylation of the *14-3-3 $\sigma$*  gene plays a role in inactivating the *p53*-dependent pathway, we examined the correlation between *14-3-3 $\sigma$*  methylation and *p53* mutations. Four of five cell lines with *14-3-3 $\sigma$*  methylation had *p53* mutations (MKN74, wild type *p53*; MKN28, Colo320DM, HLE, and HuH7, mutated *p53*), and six of seven cell lines without *14-3-3 $\sigma$*  methylation had *p53* mutations (MKN45, wild-type *p53*; MKN7, NUGC3, DLD1, HT29, Colo201, and PLC/PRF/5, mutated *p53*). There was no difference in the frequency of *p53* mutations between methylated and unmethylated cell lines. However, in primary GCs, *p53* mutations were found at a lower frequency in *14-3-3 $\sigma$*  methylated cases (1 of 16 versus 6 of 16,  $P = 0.03$ ; data not shown).

## Discussion

In the present study, we demonstrated that aberrant hypermethylation of the 5' region of *14-3-3 $\sigma$*  was detected in cell lines from various tissue types and in a subset of primary GC tissues. Aberrant methylation of the 5' region of *14-3-3 $\sigma$*  correlated well with loss of expression, and treatment with the methyltransferase inhibitor 5-aza-2'-deoxycytidine induced demethylation and reexpression of the gene. Loss of expression of *14-3-3 $\sigma$*  mRNA was also found in xenografts from GC with methylation, suggesting that aberrant methylation of the 5' CpG island of *14-3-3 $\sigma$*  plays a role in silencing this gene.

Much evidence has shown that 14-3-3 proteins are involved in  $G_2$ -M-phase progression as well as in signal transductions that lead to apoptosis, and it is strongly postulated that the inactivation of *14-3-3 $\sigma$*  might play an important role in tumor progression. Ostergaard *et al.* (8) showed that less-differentiated bladder squamous cell carcinoma is characterized by decreased expression of some proteins, including *14-3-3 $\sigma$* . In the present study, *14-3-3 $\sigma$*  methylation was frequently observed in poorly differentiated adenocarcinomas. These results suggest that decreased expression of *14-3-3 $\sigma$*  is associated with the development of undifferentiated GCs. Recently, Melis and White (15) also demonstrated decreased expression of *14-3-3 $\sigma$*  in colonic polyps. Thus, *14-3-3 $\sigma$*  inactivation may be widely seen in human neoplasias of various origins, although the association between inactivation and the role in cancer development should be further investigated. Because methylation of multiple CpG islands has often been observed in a subset of CRCs (16) and GCs (17), methylation of *14-3-3 $\sigma$*  may be involved in a "hypermethylator phenotype." In fact, GC cases with

14-3-3 $\sigma$  methylation showed methylation of several other loci, including *p16*, *hMLH1*, and *E-cadherin*.<sup>4</sup>

It is also interesting that undifferentiated GC rarely showed *p53* mutations, and this could be partially explained by epigenetic inactivation of 14-3-3 $\sigma$ , which is one of the downstream target genes of *p53* (9). Inactivation of 14-3-3 $\sigma$  by methylation in cancers may lead to impairment of part of the *p53* function. Recent studies have indicated that aberrant G<sub>2</sub> checkpoint control causes genetic instability in neoplasia (18). Cahill *et al.* (19) demonstrated mutations of mitotic checkpoint genes, *hBUB1* and *hBUBR1*, in CRCs with CIN. Although a high proportion of human cancers are likely to have a CIN phenotype, mutations of the genes involving the G<sub>2</sub>-M-phase checkpoint have rarely been found, and the mechanism of CIN in most of them is still unknown. It is not clear whether 14-3-3 $\sigma$  inactivation can cause genetic instability in cancers, but two GC cell lines with 14-3-3 $\sigma$  methylation showed the CIN phenotype by fluorescence *in situ* hybridization analysis (data not shown). Further study on the correlation between genetic instability and 14-3-3 $\sigma$  is needed.

From the results of the flow cytometry analysis, after treatment with a DNA-damaging agent, the G<sub>2</sub> checkpoint appears to be impaired in cell lines with 14-3-3 $\sigma$  methylation. MKN74, which showed methylation of 14-3-3 $\sigma$ , failed to arrest at G<sub>2</sub>-M phase and underwent apoptosis, which seems to be consistent with the findings in a recent study by Chan *et al.* (10) In contrast, MKN45 and MKN7, which did not show methylation of 14-3-3 $\sigma$ , arrested at G<sub>2</sub>, indicating that DNA-damaging agents are more effective in cancers with 14-3-3 $\sigma$  methylation. MKN7 (with mutated *p53*) initially showed a slight increase in 14-3-3 $\sigma$  mRNA expression after treatment but subsequently showed reduced expression and incomplete G<sub>2</sub> arrest. The incomplete induction of 14-3-3 $\sigma$  in MKN7 seems to be due to the impairment of *p53* function. These results indicated that 14-3-3 $\sigma$  inactivation could be achieved by either mutation of *p53* or methylation of 14-3-3 $\sigma$ . Pretreatment with 5-aza-2'-deoxycytidine before Adriamycin treatment was performed to analyze the effect of the reexpressed 14-3-3 $\sigma$  gene in the methylated cells. Restoration of G<sub>2</sub> arrest by DNA damage after 5-aza-2'-deoxycytidine treatments was present in the cell lines. However, the genes induced by 5-aza-2'-deoxycytidine are not limited to 14-3-3 $\sigma$ , and the involvement of many unknown genes that were inactivated by demethylation should be considered; further study is necessary to analyze this issue from different aspects.

In conclusion, we demonstrated that inactivation of the 14-3-3 $\sigma$  gene is associated with 5' CpG island hypermethylation in human cancers. To our knowledge, this is the first report on epigenetic silencing of the G<sub>2</sub> checkpoint gene in human neoplasia. Our results indicate that epigenetic changes can induce further genetic alterations. GC cases with 14-3-3 $\sigma$  methylation may be a good target for treatment with chemotherapeutic agents. Although much remains to be clarified regarding aberrant methylation of 14-3-3 $\sigma$ , further study should shed light on the mechanism of cancer development as well as more effective cancer therapies.

<sup>4</sup> H. Suzuki *et al.*, Concordant methylation of multiple genes in gastric cancer, manuscript in preparation.

## Acknowledgments

We thank Drs. Hiroaki Mita and Masanobu Kusano for collecting GC tissues. We also thank Dr. Jean-Pierre Issa for critical review of the manuscript.

## References

- Zha, J., Harada, H., Yang, E., Jochel, J., and Korsmeyer, S. J. Serine phosphorylation of death agonist BAD in response to survival factor results in binding to 14-3-3 not BCL-X<sub>L</sub>. *Cell*, 87: 619–628, 1996.
- Datta, S. P., Dudek, H., Tao, X., Masters, S., Fu, H., Gotoh, Y., and Greenberg, M. E. Akt phosphorylation of BAD couples survival signals to the cell-intrinsic death machinery. *Cell*, 91: 231–241, 1997.
- Peng, C.-Y., Graves, P. R., Thoma, R. S., Wu, Z., Shaw, A. S., and Piwnicka-Worms, H. Mitotic and G<sub>2</sub> checkpoint control: regulation of 14-3-3 protein binding by phosphorylation of Cdc25C on serine-216. *Science (Washington DC)*, 277: 1501–1505, 1997.
- Lopez-Girona, A., Furnari, B., Mondesert, O., and Russel, P. Nuclear localization of Cdc25C is regulated by DNA damage and a 14-3-3 protein. *Nature (Lond.)*, 397: 172–175, 1999.
- Leffers, H., Madsen, P., Rasmussen, H. H., Honore, B., Andersen, A. H., Walbum, E., Vandekerckhove, J., and Celis, J. E. Molecular cloning and expression of the transformation sensitive epithelial marker stratifin. A member of a protein kinase C signaling pathway. *J. Mol. Biol.*, 231: 982–998, 1993.
- Vellucci, V. F., Germino, F. J., and Reiss, M. Cloning of putative growth regulatory genes from primary human keratinocytes by subtractive hybridization. *Gene (Amst.)*, 166: 213–220, 1995.
- Dellambra, E., Patrone, M., Sparatore, B., Negri, A., Ceciliani, F., Bondanza, S., Molina, F., Cancedda, F. D., and De Luca, M. Stratifin, a keratinocyte specific 14-3-3 protein, harbors a pleckstrin homology (PH) domain and enhances protein kinase C activity. *J. Cell Sci.*, 108: 3569–3579, 1995.
- Ostergaard, M., Rasmussen, H. H., Nielsen, H. V., Vorum, H., Orntoft, T. F., Wolf, H., and Celis, J. E. Proteome profiling of bladder squamous cell carcinomas: identification of markers that define their degree of differentiation. *Cancer Res.*, 57: 4111–4117, 1997.
- Hermeking, H., Lengauer, C., Polyak, K., He, T.-C., Zhang, L., Thiagalingam, S., Kinzler, K. W., and Vogelstein, B. 14-3-3 $\sigma$  is a p53-regulated inhibitor of G<sub>2</sub>/M progression. *Mol. Cell*, 1: 3–11, 1997.
- Chan, T. A., Hermeking, H., Lengauer, C., Kinzler, K. W., and Vogelstein, B. 14-3-3 $\sigma$  is required to prevent mitotic catastrophe after DNA damage. *Nature (Lond.)*, 401: 616–620, 1999.
- Suzuki, H., Itoh, F., Toyota, M., Kikuchi, T., Kakiuchi, H., Hinoda, Y., and Imai, K. Quantitative DNA methylation analysis by fluorescent polymerase chain reaction single-strand conformation polymorphism using an automated DNA sequencer. *Electrophoresis*, 20: 904–908, 2000.
- Herman, J. G., Graff, J. R., Myohanen, S., Nelkin, B. D., and Baylin, S. B. Methylation-specific PCR: a novel PCR assay for methylation status of CpG islands. *Proc. Natl. Acad. Sci. USA*, 93: 9821–9826, 1996.
- Rhei, E., Bogomolny, F., Federici, M. G., Maresco, D. L., Offit, K., Robson, M. E., Saigo, P. E., and Boyd, J. Molecular genetic characterization of BRCA1- and BRCA2-linked hereditary ovarian cancers. *Cancer Res.*, 58: 3193–3196, 1999.
- Gardiner-Garden, M., and Frommer, M. CpG islands in vertebrate genomes. *J. Mol. Biol.*, 196: 261–282, 1987.
- Melis, R., and White R. Characterization of colonic polyps by two-dimensional gel electrophoresis. *Electrophoresis*, 20: 1055–1064, 1999.
- Toyota, M., Ahuja, N., Ohe-Toyota, M., Herman, J. G., Baylin, S. B., and Issa, J. P. J. CpG island methylator phenotype in colorectal cancer. *Proc. Natl. Acad. Sci. USA*, 96: 8681–8686, 1999.
- Toyota, M., Ahuja, N., Suzuki, H., Itoh, F., Ohe-Toyota, M., Imai, K., Baylin, S. B., and Issa, J. P. J. Aberrant methylation in gastric cancer associated with the CpG island methylator phenotype. *Cancer Res.*, 59: 5438–5442, 1999.
- Lengauer, C., Kinzler, K. W., and Vogelstein, B. Genetic instability in human cancers. *Nature (Lond.)*, 396: 643–649, 1999.
- Cahill, P. D., Lengauer, C., Yu, J., Riggins, G. J., Willson, J. K. V., Markowitz, S. D., Kinzler, K. W., and Vogelstein, B. Mutations of mitotic checkpoint genes in human cancers. *Nature (Lond.)*, 392: 300–303, 1999.